IEEE Access
Multidisciplinary ⁝ Rapid Review ⁝ Open Access Journal

Received January 8, 2019, accepted January 21, 2019, date of publication February 1, 2019, date of current version March 20, 2019.

Digital Object Identifier 10.1109/ACCESS.2019.2897015

Adaptive Terminal Sliding Mode Control for Hybrid Energy Storage Systems of Fuel Cell, Battery and Supercapacitor

DEZHI XU, (Member, IEEE), QIAN LIU, WENXU YAN, (Member, IEEE), AND WEILIN YANG, (Member, IEEE)

School of Internet of Things Engineering, Jiangnan University, Wuxi 214122, China

Corresponding author: Dezhi Xu (lutxdz@126.com)

This work was supported in part by the National Natural Science Foundation of China under Grant 61503156, in part by the National Key Research and Development Program under Grant 2016YFD0400301, in part by the Open Research Fund of Jiangsu Collaborative Innovation Center for Smart Distribution Network, Nanjing Institute of Technology, under Grant XTCX201806, in part by the National First-Class Discipline Program of Food Science and Technology under Grant JUFSTR20180205, and in part by the State Grid Zhejiang Province Technology Project under Grant SGTYHT/17-JS-201.

ABSTRACT In this paper, a terminal sliding mode control strategy with projection operator adaptive law is proposed in a hybrid energy storage system (HESS). The objective of the proposed control strategy is to provide power for load in time, get good tracking performance of the current of the fuel cell, battery, and supercapacitor, and obtain a stable voltage of the dc bus. At first, the topological structure of the system is proposed, and the mathematical models are derived. Then, on the basis of the working characteristics of the energy storage unit, the load power is reasonably and effectively distributed to increase the service life of HESS and improve energy efficiency. Meanwhile, according to the tracking errors of reference and actual values, the terminal sliding surfaces can be set out. The controller can be designed by the constraint condition, combining the projection operator adaptive law. In addition, the HESS with the proposed control is proved to be asymptotically stable by using the Lyapunov method. Finally, the simulation results show that the proposed control strategy can make the whole system stable, and the control objective can also be better realized.

INDEX TERMS Fuel cell, battery, supercapacitor, hybrid energy storage system, projection adaptive, terminal sliding mode control.

I. INTRODUCTION

Nowadays, in a serious condition of increasing tension over energy, conventional sources of energy are declining sharply, like fossil fuels, while clean energy has tough problems with high-cost and intermittent [1]–[4]. To achieve a low carbon economy, the effective utilization of traditional energy and clean energy, or the energy transfer and storage after utilization, are the key research directions. It is against this background that energy storage is believed to be essential in the energy supply chain. Energy storage can help to plug the leakages, compensate the fluctuating power of distributed renewable energy in an active stabilizing way and improve the reliability and stability of power supply. As a result, as an important research direction of energy utilization, energy storage has recently attracted the attention of governments, researchers, stakeholders and investors [5]–[7].

Now the function positioning of energy storage unit (ESU) is not clear and there is no generally accepted standards, at the same time, some of the energy storage device also does not have clear distinction. Therefore, it is difficult for a single type of energy storage to meet all the demands of load requirements. It is the current technical trend to develop hybrid energy storage system (HESS) by utilizing the complementary characteristics of different energy storage. HESSs are widely used in photovoltaic power generation system, wind-solar complementary micro grid and electric vehicle, etc. For example, in [8], the hybrid electric vehicle technology is the result of the desire to have vehicles with a better fuel economy and lower tailpipe emissions to meet the

The associate editor coordinating the review of this manuscript and approving it for publication was Jianyong Yao.

requirements of environmental policies as well as to absorb the impact of rising fuel prices. But most HESSs are mainly based on subjective judgement and experience [9]–[12].

Mainstream hybrid energy storage systems include fuel cells-supercapacitors, batteries-supercapacitors, fuel cells-batteries-supercapacitors, etc [13]–[19]. The storage system consists of a fuel cell (FC), serving as the main power source, and a supercapacitor (SC), serving as an auxiliary power source [15], but the excess energy of fuel cell cannot be recycled well; although fuel cell is clean energy, it cannot be reused as a disposable energy, which makes the system limited in many cases. The system of battery-SC hybrid energy storage is used in [16] and [17]. However, reducing cost and increasing energy density are two barriers for widespread application of lithium-ion batteries [18]. In [19] and [20], the model of hybrid energy storage system can be referenced, which is made up of three ESUs. This model can combine the advantages of the three energy storage devices, that allocating energy efficiently and reasonably according to load condition.

Recently, many control methods and strategies of HESS are put forward. In [19], a dynamic model of the system is developed, which is based on the nonlinear behavior of power sources and converters, and nonlinear control is proposed. In [20], a multiple-input power electronic converter is designed to be used in an electric vehicle propulsion system. In [21], a novel adaptive control strategy based on input/output data is proposed in this paper to solve the problem of power management of battery energy storage system. There are also droop control and model-free methods that can be referred to [22]–[24]. However, the hybrid energy storage studied in this paper does not involve distributed energy storage and grid-connection, energy distribution and control strategy are the significant points. In order to control the nonlinear system better, sliding mode control is improved and adopted [25]–[29]. To obtain better performance, terminal sliding mode control is mainly used to make the state tracking errors converge to zero in finite time [27], [28]. For unknown bounded parameters in the system, it is necessary to estimate them dynamically, so the adaptive law of the projection operator can be used [30]–[33], further applications can refer to [34]–[36]. In addition, the combination of adaptive and nonlinear control can be referred to [37] and [38].

In this paper, a terminal sliding mode control strategy of projection operator adaptive law is proposed in HESS system. The objective of the proposed controller is to provide power to load power in time, get good tracking performance of the current of three ESUs, and obtain stable voltage of the DC bus. Three DC-DC converters are used to transform the FC-battery-SC current and voltage. Based on the proposed power distribution scheme, the power of three parts can be obtained, which provides reference current for the circuit. According to the errors of referential and actual values, the terminal sliding surface can be set out. The part relating to resistances, inductances, and capacitances can be expressed by projection operator, that an adaptive law can be introduced. From the constraint condition of controller, the controller can be obtained. The HESS with the proposed adaptive terminal sliding mode control is proved to be asymptotically stable, combining the projection operator adaptive law and Lyapunov function. The proposed control scheme can achieve the contributions summarized as:

1) According to the physical characteristics and load power, FC, battery and SC are effectively used by power distribution strategy.
2) No specific model parameters are involved in the design of the controller. The unknown model parameters can be bounded and estimated dynamically by projection operator adaptive law.
3) Terminal sliding mode control is used to make the state tracking errors converge to zero in finite time.
4) The controller can be designed by the constraint condition. And the HESS is asymptotically stable by Lyapunov function verification.

This paper is organized as follows: In Section II, the HESS modeling is illustrated. In Section III, the proposed control strategy is summarized, which includes two parts, power distribution strategy and adaptive terminal sliding mode control strategy. In Section IV, simulink results and analysis are given to verify the validity of the designed controller. Conclusions are presented in Section V.

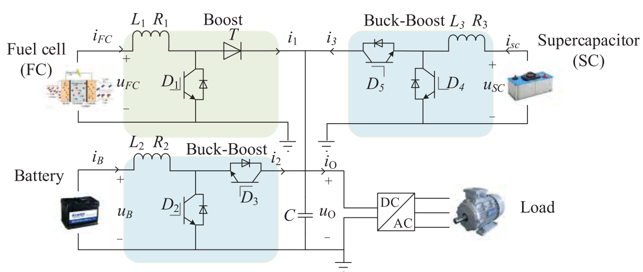

FIGURE 1. Circuit topology of the hybrid energy storage system.

II. THE HESS MODELING

In Figure 1, the topological structure of the HESS is clearly designed. The HESS employs a boost converter, two buck-boost converters and an additional control circuit. The control circuit makes the best power partition under the effective strategy. Both fuel cell and battery are main energy component, and they work on different load power condition. Meanwhile, both battery and supercapacitor are the energy storage device. When the fuel cell works at low efficiency, or in failure mode, or the load charges the system, the battery is the dominant part. Because of the physical properties, the peak power which the FC and battery cannot offer can be gained by SC. The boost converter consists of an insulated gate bipolar transistor (IGBT), a diode T, a filtering capacitor C and a high-frequency inductor L_1. While the bi-directional DC-DC converter includes two IGBTs and a high-frequency filtering inductor. The output currents of boost converter and the buck-boost converters are through the capacitor and linked to a DC-AC converter, which passed to the load.

A. MODEL OF FUEL CELL OPERATION

Applying Kirchhoff's law to the part of fuel cell and boost converter, the equations can be obtained as:

$$\frac{di_{FC}}{dt} = -\frac{R_1}{L_1}i_{FC}+\frac{1}{L_1}u_{FC} - \frac{1-m_1}{L_1}u_O \quad (1)$$
$$i_1 = (1-m_1)i_{FC} \quad (2)$$

where the symbol m_1 means the duty cycle of the IGBT D_1, which varies from 1 to 0.

B. MODEL OF BATTERY OPERATION

In consideration of the characteristic of battery, the auxiliary power section can be divided into two work states, discharge state and charge state. If the battery works on discharge state, m_3 is limited to 0 and m_2 takes the value from 1 to 0. When it works on the charge state, m_2 is set to 0, and m_3 varies from 1 to 0. The relationship of charge state can be written as:

$$i_B^* > 0 \quad (3)$$
$$\frac{di_B}{dt} = -\frac{R_2}{L_2}i_B + \frac{1}{L_2}u_B - \frac{1-m_2}{L_2}u_O \quad (4)$$
$$i_2 = (1-m_2)i_B \quad (5)$$

where i_B^* represents the battery current reference.

The discharge state of battery can be obtained by:

$$i_B^* < 0 \quad (6)$$
$$\frac{di_B}{dt} = -\frac{R_2}{L_2}i_B + \frac{1}{L_2}u_B - \frac{m_3}{L_2}u_O \quad (7)$$
$$i_2 = m_3 i_B \quad (8)$$

Then combining the above equations, the model of the battery operation can be gained as follows:

$$m_{23} = \begin{cases} 1-m_2 & i_B^* > 0 \\ m_3 & i_B^* < 0 \end{cases} \quad (9)$$
$$\frac{di_B}{dt} = -\frac{R_2}{L_2}i_B + \frac{1}{L_2}u_B - \frac{m_{23}}{L_2}u_O \quad (10)$$
$$i_2 = m_{23} i_B \quad (11)$$

C. MODEL OF SUPERCAPACITOR OPERATION

As same with the charging and discharging states of battery, the equations of supercapacitor can be obtained:

$$m_{45} = \begin{cases} 1-m_4 & i_{SC}^* > 0 \\ m_5 & i_{SC}^* < 0 \end{cases} \quad (12)$$
$$\frac{di_{SC}}{dt} = -\frac{R_3}{L_3}i_{SC} + \frac{1}{L_3}u_{SC} - \frac{m_{45}}{L_3}u_O \quad (13)$$
$$i_3 = m_{45} i_{SC} \quad (14)$$

where i_{SC}^* means the current reference of supercapacitor, which can be explained in detail later.

D. MODEL OF HYBRID ENERGY STORAGE SYSTEM

From Kirchhoff's law of current, one can easily obtained:

$$\frac{du_O}{dt} = \frac{1-m_1}{C}i_{FC} + \frac{m_{23}}{C}i_B + \frac{m_{45}}{C}i_{SC} - \frac{1}{C}i_O \quad (15)$$

From equations (1), (10), (13) and (15), complete dynamic mathematical model can be obtained:

$$\frac{di_{FC}}{dt} = -\frac{R_1}{L_1}i_{FC} + \frac{1}{L_1}u_{FC} - \frac{1-m_1}{L_1}u_O \quad (16)$$
$$\frac{di_B}{dt} = -\frac{R_2}{L_2}i_B + \frac{1}{L_2}u_B - \frac{m_{23}}{L_2}u_O \quad (17)$$
$$\frac{di_{SC}}{dt} = -\frac{R_3}{L_3}i_{SC} + \frac{1}{L_3}u_{SC} - \frac{m_{45}}{L_3}u_O \quad (18)$$
$$\frac{du_O}{dt} = \frac{1-m_1}{C}i_{FC} + \frac{m_{23}}{C}i_B + \frac{m_{45}}{C}i_{SC} - \frac{1}{C}i_O \quad (19)$$

The parameters R_1, R_2, R_3, L_1, L_2, L_3 and C used in the HESS is hard to get precisely in practice. Considering these parameters as unknowns and incorporating them in the design procedure of the adaptive controller, the unknown parameters in the HESS model can be defined as follows:

$$\sigma_1 = \frac{1}{L_1} = \frac{1}{L_2} = \frac{1}{L_3} \quad (20)$$
$$\sigma_2 = \frac{R_1}{L_1} = \frac{R_2}{L_2} = \frac{R_3}{L_3} \quad (21)$$
$$\sigma_3 = \frac{1}{C} \quad (22)$$

Put the unknown parameters into the model (20), (21) and (22), the HESS modeling can be simplified as

$$\frac{dX_1}{dt} = -\sigma_2 X_1 - (1-m_1)\sigma_1 X_4 + \sigma_1 u_{FC} \quad (23)$$
$$\frac{dX_2}{dt} = -\sigma_2 X_2 - m_{23}\sigma_1 X_4 + \sigma_1 u_B \quad (24)$$
$$\frac{dX_3}{dt} = -\sigma_2 X_3 - m_{45}\sigma_1 X_4 + \sigma_1 u_{SC} \quad (25)$$
$$\frac{dX_4}{dt} = (1-m_1)\sigma_3 X_1 + m_{23}\sigma_3 X_2 + m_{45}\sigma_3 X_3 - \sigma_3 i_O \quad (26)$$

where X_1, X_2, X_3 and X_4 mean i_{FC}, i_B, i_{SC} and u_O, respectively.

In model (23), (24), (25) and (26), the HESS is obviously MOMI nonlinear system, so it is necessary to design an effective control strategy. By effectively controlling for m_1, m_{23} and m_{45}, the model (23) - (26) can reliability operate, i_{FC}, i_B, i_{SC} and u_O can meet the requirements. In addition, effective PWM waves can be provided to the HESS by controller.

III. DESIGN OF CONTROL STRATEGY

A. POWER DISTRIBUTION STRATEGY

According to the performance characteristics of fuel cell, battery and supercapacitor, the power distribution management can be designed appropriately. Fuel cell has high energy density but is low-efficiency in light load situations, so the fuel cell provides primary energy in the situation when the load is medium-heavy and long-time. When the time of the load is short and the weight is relatively light, the battery plays the main role. The battery is used as the long-term energy storage, which can be recharged in cycles. While the supercapacitor has high power density, this makes the obvious advantage for SC in supplying peak power in the state of acceleration and high load.

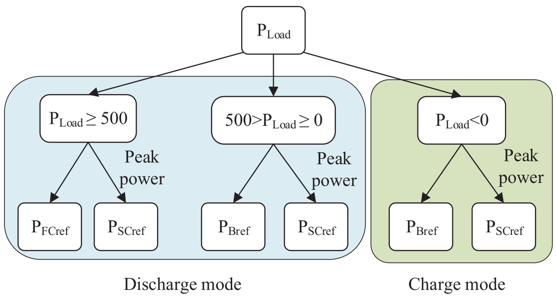

FIGURE 2. Schematic diagram of power distribution.

When the load power P_{Load} is positive, it divides into above cases. When P_{Load} is negative, this means the fuel cell does not work, the battery and SC can recover the regenerative braking energy. The battery will be charged, and the SC will provide peak power. The details of power flow are shown in figure 2.

Meanwhile, the power distribution can be achieved as:

$$P_{FCref} + P_{Bref} + P_{SCref} = P_{Load} \tag{27}$$

where P_{Load} is the load required power, P_{FCref} and P_{Bref} are fuel cell and battery reference power, respectively, which are set in power distribution strategy. P_{SCref} means the reference power of supercapacitor that comes from the remaining load required power, which consists of high frequency peak power and the energy produced by regenerative braking. Therefore, the current reference of FC, battery and SC can be obtained:

$$i_{FC}^{*} = \frac{P_{FCref}}{u_{FC}} \tag{28}$$

$$i_{B}^{*} = \frac{P_{Bref}}{u_{B}} \tag{29}$$

$$i_{SC}^{*} = \frac{P_{SCref}}{u_{SC}} \tag{30}$$

B. ADAPTIVE TERMINAL SLIDING MODE CONTROL STRATEGY

The power distribution strategy can be seen in the upper part, and in the paper, we take i_{FC}, i_B, i_{SC} and u_O as control objects directly. The design procedure of the proposed controller for HESS is shown as follows. Define the tracking error variables e_1, e_2, e_3 and e_4 as:

$$e_1 = X_1 - i_{FC}^{*} \tag{31}$$

$$e_2 = X_2 - i_{B}^{*} \tag{32}$$

$$e_3 = X_3 - i_{SC}^{*} \tag{33}$$

$$e_4 = X_4 - u_{O}^{*} \tag{34}$$

where u_O^* represents the desired value of u_O, and will be introduced later.

Defining the terminal sliding mode surface:

$$s_1 = e_1 + k_1\left(\int_{0-}^{t} e_1 dt\right)^{p_1/q_1} \tag{35}$$

$$s_2 = e_2 + k_2\left(\int_{0-}^{t} e_2 dt\right)^{p_2/q_2} \tag{36}$$

$$s_3 = e_3 + k_3\left(\int_{0-}^{t} e_3 dt\right)^{p_3/q_3} \tag{37}$$

$$s_4 = e_4 + k_4\left(\int_{0-}^{t} e_4 dt\right)^{p_4/q_4} \tag{38}$$

where $k_1 > 0$, $k_2 > 0$, $k_3 > 0$ and $k_4 > 0$ are the designed constants of sliding mode surface, p_1, p_2, p_3, p_4, q_1, q_2, q_3 and q_4 are the positive odd numbers, which $1 < p_1/q_1 < 2$, $1 < p_2/q_2 < 2$, $1 < p_3/q_3 < 2$, $1 < p_4/q_4 < 2$.

The derivative of equation (34), (35), (36) and (37) can be calculated as:

$$\dot{s}_1 = \dot{e}_1 + k_1\left(\frac{p_1}{q_1}\right)e_1\left(\int_{0-}^{t} e_1 dt\right)^{p_1/q_1-1} \tag{39}$$

$$\dot{s}_2 = \dot{e}_2 + k_2\left(\frac{p_2}{q_2}\right)e_2\left(\int_{0-}^{t} e_2 dt\right)^{p_2/q_2-1} \tag{40}$$

$$\dot{s}_3 = \dot{e}_3 + k_3\left(\frac{p_3}{q_3}\right)e_3\left(\int_{0-}^{t} e_3 dt\right)^{p_3/q_3-1} \tag{41}$$

$$\dot{s}_4 = \dot{e}_4 + k_4\left(\frac{p_4}{q_4}\right)e_4\left(\int_{0-}^{t} e_4 dt\right)^{p_4/q_4-1} \tag{42}$$

Defining the adaptive estimation error:

$$\tilde{\sigma}_i = \hat{\sigma}_i - \sigma_i, \quad i = 1, 2, 3 \tag{43}$$

where σ_i is the parameter value of adaptive estimation.

Combining the above equations, the new equations can be calculated as:

$$\dot{s}_1 = -\sigma_2 X_1 - (1-m_1)\sigma_1 X_4 + \sigma_1 u_{FC} - \dot{i}_{FC}^{*} + k_1\left(\frac{p_1}{q_1}\right)e_1\left(\int_{0-}^{t} e_1 dt\right)^{p_1/q_1-1} \tag{44}$$

$$\dot{s}_2 = -\sigma_2 X_2 - m_{23}\sigma_1 X_4 + \sigma_1 u_B - \dot{i}_{B}^{*} + k_2\left(\frac{p_2}{q_2}\right)e_2\left(\int_{0-}^{t} e_2 dt\right)^{p_2/q_2-1} \tag{45}$$

$$\dot{s}_3 = -\sigma_2 X_3 - m_{45}\sigma_1 X_4 + \sigma_1 u_{SC} - \dot{i}_{SC}^{*} + k_3\left(\frac{p_2}{q_2}\right)e_3\left(\int_{0-}^{t} e_3 dt\right)^{p_3/q_3-1} \tag{46}$$

$$\dot{s}_4 = (1-m_1)\sigma_3 X_1 + m_{23}\sigma_3 X_2 + m_{45}\sigma_3 X_3 - \sigma_3 i_O - \dot{u}_{O}^{*} + k_4\left(\frac{p_4}{q_4}\right)e_4\left(\int_{0-}^{t} e_4 dt\right)^{p_4/q_4-1} \tag{47}$$

To prove the stability of the system, the Lyapunov function is designed as:

$$V = \frac{1}{2}{s_1}^2 + \frac{1}{2}{s_2}^2 + \frac{1}{2}{s_3}^2 + \frac{1}{2}{s_4}^2 + \frac{1}{2}\frac{\tilde{\sigma}_1^2}{r_1} + \frac{1}{2}\frac{\tilde{\sigma}_2^2}{r_2} + \frac{1}{2}\frac{\tilde{\sigma}_3^2}{r_3} \tag{48}$$

where s_4 can be expressed by adaptive estimation error parameter σ_3.

Substituting the values of $\dot{s}_1, \dot{s}_2, \dot{s}_3$ and $\dot{s}_4$, the derivative of the Lyapunov function with respect to time can be obtained:

$$\begin{aligned}
\dot{V} &= s_1\dot{s}_1+s_2\dot{s}_2+s_3\dot{s}_3+s_4\dot{s}_4+\frac{1}{r_1}\tilde{\sigma}_1\dot{\tilde{\sigma}}_1+\frac{1}{r_2}\tilde{\sigma}_2\dot{\tilde{\sigma}}_2+\frac{1}{r_3}\tilde{\sigma}_3\dot{\tilde{\sigma}}_3 \\
&= s_1\dot{s}_1+s_2\dot{s}_2+s_3\dot{s}_3+s_4\dot{s}_4+\frac{1}{r_1}\tilde{\sigma}_1\dot{\hat{\sigma}}_1+\frac{1}{r_2}\tilde{\sigma}_2\dot{\hat{\sigma}}_2+\frac{1}{r_3}\tilde{\sigma}_3\dot{\hat{\sigma}}_3 \\
&= s_1\Big(-\hat{\sigma}_2X_1-(1-m_1)\hat{\sigma}_1X_4+\hat{\sigma}_1u_{FC}-\dot{i}^*_{FC} \\
&\quad +k_1\Big(\frac{p_1}{q_1}\Big)e_1\Big(\int_{0-}^{t}e_1dt\Big)^{p_1/q_1-1}\Big) \\
&\quad +s_2\Big(-\hat{\sigma}_2X_2-m_{23}\hat{\sigma}_1X_4+\hat{\sigma}_1u_B-\dot{i}^*_B \\
&\quad +k_2\Big(\frac{p_2}{q_2}\Big)e_2\Big(\int_{0-}^{t}e_2dt\Big)^{p_2/q_2-1}\Big) \\
&\quad +s_3\Big(-\hat{\sigma}_2X_3-m_{45}\hat{\sigma}_1X_4+\hat{\sigma}_1u_{SC}-\dot{i}^*_{SC} \\
&\quad +k_3\Big(\frac{p_3}{q_3}\Big)e_3\Big(\int_{0-}^{t}e_3dt\Big)^{p_3/q_3-1}\Big) \\
&\quad +s_4\Big((1-m_1)\hat{\sigma}_3X_1+m_{23}\hat{\sigma}_3X_2+m_{45}\hat{\sigma}_3X_3-\hat{\sigma}_3i_O \\
&\quad -\dot{u}^*_O+k_4\Big(\frac{p_4}{q_4}\Big)e_4\Big(\int_{0-}^{t}e_4dt\Big)^{p_4/q_4-1}\Big) \\
&\quad +\tilde{\sigma}_1\Big(\frac{1}{r_1}\dot{\hat{\sigma}}_1+s_1\big((1-m_1)X_4-u_{FC}\big) \\
&\quad +s_2(m_{23}X_4-u_B)+s_3(m_{45}X_4-u_{SC})\Big) \\
&\quad +\tilde{\sigma}_2\Big(\frac{1}{r_2}\dot{\hat{\sigma}}_2+s_1X_1+s_2X_2+s_3X_3\Big) \\
&\quad +\tilde{\sigma}_3\Big(\frac{1}{r_3}\dot{\hat{\sigma}}_3+s_4\big(-(1-m_1)X_1 \\
&\quad -m_{23}X_2-m_{45}X_3+i_O\big)\Big)
\end{aligned} \tag{49}$$

Considering the boundedness of parameter estimation, so in $\dot{V}$, the adaptive update laws are designed as:

$$\begin{aligned}
\dot{\hat{\sigma}}_1 &= r_1proj\Big(\hat{\sigma}_1, -s_1\big((1-m_1)X_4-u_{FC}\big) \\
&\qquad -s_2(m_{23}X_4-u_B)-s_3(m_{45}X_4-u_{SC})\Big)
\end{aligned} \tag{50}$$

$$\dot{\hat{\sigma}}_2 = r_2proj\Big(\hat{\sigma}_2, -s_1X_1-s_2X_2-s_3X_3\Big) \tag{51}$$

$$\begin{aligned}
\dot{\hat{\sigma}}_3 &= r_3proj\Big(\hat{\sigma}_3, -s_4\big(-(1-m_1)X_1-m_{23}X_2 \\
&\qquad -m_{45}X_3+i_O\big)\Big)
\end{aligned} \tag{52}$$

where function $proj(\cdot)$ represents the projection operator which guarantee the bounds of parameters estimation [34]–[36]. The adaptive law with the discontinuous projection operator is designed as:

$$proj(\hat{\psi},\tau) = \begin{cases} 0, & if\ \hat{\psi}=\hat{\psi}_{\max}\ and\ \tau>0 \\ 0, & if\ \hat{\psi}=\hat{\psi}_{\max}\ and\ \tau<0 \\ \tau, & otherwise \end{cases} \tag{53}$$

where $\hat{\psi}_{\max}$ represents the upper limit of the estimated value of $\hat{\psi}$. And the conclusions of the projection operator can be written as:

$$\begin{aligned}
&Property1 \quad \hat{\psi}\in\Omega_\psi \triangleq \Big\{\hat{\psi}:\psi_{\min}\le\hat{\psi}\le\psi_{\max}\Big\} \\
&Property2 \quad \tilde{\psi}\Big[proj(\hat{\psi},\tau)-\tau\Big]\le 0,\ \forall\tau
\end{aligned} \tag{54}$$

Taking equation (50), (51), (52) into (49), equation (49) can be simplified as:

$$\begin{aligned}
\dot{V} &\le s_1\Big(-\hat{\sigma}_2X_1-(1-m_1)\hat{\sigma}_1X_4+\hat{\sigma}_1u_{FC}-\dot{i}^*_{FC} \\
&\quad +k_1\Big(\frac{p_1}{q_1}\Big)e_1\Big(\int_{0-}^{t}e_1dt\Big)^{p_1/q_1-1}\Big) \\
&\quad +s_2\Big(-\hat{\sigma}_2X_2-m_{23}\hat{\sigma}_1X_4+\hat{\sigma}_1u_B-\dot{i}^*_B \\
&\quad +k_2\Big(\frac{p_2}{q_2}\Big)e_2\Big(\int_{0-}^{t}e_2dt\Big)^{p_2/q_2-1}\Big) \\
&\quad +s_3\Big(-\hat{\sigma}_2X_3-m_{45}\hat{\sigma}_1X_4+\hat{\sigma}_1u_{SC}-\dot{i}^*_{SC} \\
&\quad +k_3\Big(\frac{p_3}{q_3}\Big)e_3\Big(\int_{0-}^{t}e_3dt\Big)^{p_3/q_3-1}\Big) \\
&\quad +s_4\Big((1-m_1)\hat{\sigma}_3X_1+m_{23}\hat{\sigma}_3X_2+m_{45}\hat{\sigma}_3X_3 \\
&\quad -\hat{\sigma}_3i_O-\dot{u}^*_O+k_4\Big(\frac{p_4}{q_4}\Big)e_4\Big(\int_{0-}^{t}e_4dt\Big)^{p_4/q_4-1}\Big)
\end{aligned} \tag{55}$$

In order to meet Lyapunov stability theory, which requires $\dot{V}\le 0$, the constraint condition of controllers can be designed as follows:

$$\begin{aligned}
-\rho_1sgn(s_1) &= -\hat{\sigma}_2X_1-(1-m_1)\hat{\sigma}_1X_4+\hat{\sigma}_1u_{FC}-\dot{i}^*_{FC} \\
&\quad +k_1\Big(\frac{p_1}{q_1}\Big)e_1\Big(\int_{0-}^{t}e_1dt\Big)^{p_1/q_1-1}
\end{aligned} \tag{56}$$

$$\begin{aligned}
-\rho_2sgn(s_2) &= -\hat{\sigma}_2X_2-m_{23}\hat{\sigma}_1X_4+\hat{\sigma}_1u_B-\dot{i}^*_B \\
&\quad +k_2\Big(\frac{p_2}{q_2}\Big)e_2\Big(\int_{0-}^{t}e_2dt\Big)^{p_2/q_2-1}
\end{aligned} \tag{57}$$

$$\begin{aligned}
-\rho_3sgn(s_3) &= -\hat{\sigma}_2X_3-m_{45}\hat{\sigma}_1X_4+\hat{\sigma}_1u_{SC}-\dot{i}^*_{SC} \\
&\quad +k_3\Big(\frac{p_3}{q_3}\Big)e_3\Big(\int_{0-}^{t}e_3dt\Big)^{p_3/q_3-1}
\end{aligned} \tag{58}$$

$$\begin{aligned}
-\rho_4sgn(s_4) &= (1-m_1)\hat{\sigma}_3X_1+m_{23}\hat{\sigma}_3X_2+m_{45}\hat{\sigma}_3X_3 \\
&\quad -\hat{\sigma}_3i_O-\dot{u}^*_O+k_4\Big(\frac{p_4}{q_4}\Big)e_4\Big(\int_{0-}^{t}e_4dt\Big)^{p_4/q_4-1}
\end{aligned} \tag{59}$$

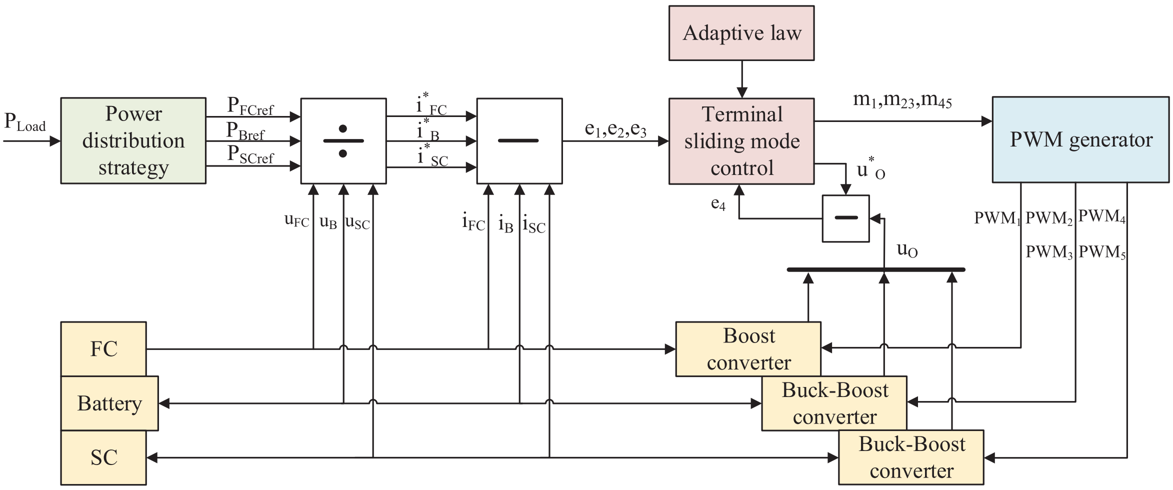

FIGURE 3. General structure diagram of HESS.

where $\rho_1 > 0$, $\rho_2 > 0$, $\rho_3 > 0$, and $\rho_4 > 0$. And $sgn(\cdot)$ means:

$$sgn(x) = \begin{cases} x/|x| & x \neq 0 \\ 0 & x = 0 \end{cases} \quad (60)$$

From equation (56), (57), (58) and (59), the controller m_1, m_{23}, m_{45} and the desired value $\dot{u}_O^*$ can be obtained:

$$m_1 = \frac{1}{\hat{\sigma}_1 X_4}\Big(-\rho_1 sgn(s_1) + \hat{\sigma}_2 X_1 - \hat{\sigma}_1 u_{FC} + \dot{i}_{FC}^* - k_1\left(\frac{p_1}{q_1}\right) e_1 \left(\int_{0-}^{t} e_1 dt\right)^{p_1/q_1 - 1}\Big) + 1 \quad (61)$$

$$m_{23} = \frac{1}{\hat{\sigma}_1 X_4}\Big(\rho_2 sgn(s_2) - \hat{\sigma}_2 X_2 + \hat{\sigma}_1 u_B - \dot{i}_B^* + k_2\left(\frac{p_2}{q_2}\right) e_2 \left(\int_{0-}^{t} e_2 dt\right)^{p_2/q_2 - 1}\Big) \quad (62)$$

$$m_{45} = \frac{1}{\hat{\sigma}_1 X_4}\Big(\rho_3 sgn(s_3) - \hat{\sigma}_2 X_3 + \hat{\sigma}_1 u_{SC} - \dot{i}_{SC}^* + k_3\left(\frac{p_3}{q_3}\right) e_3 \left(\int_{0-}^{t} e_3 dt\right)^{p_3/q_3 - 1}\Big) \quad (63)$$

$$\dot{u}_O^* = \rho_4 sgn(s_4) + \big((1 - m_1) X_1 + m_{23} X_2 + m_{45} X_3 - i_O\big)\hat{\sigma}_3 + k_4\left(\frac{p_4}{q_4}\right) e_4 \left(\int_{0-}^{t} e_4 dt\right)^{p_4/q_4 - 1} \quad (64)$$

Putting equation (56) - (59) into inequation (55) and considering the properties of $sgn(\cdot)$, inequation (55) can be simplified as:

$$\dot{V} \leq -\rho_1 |s_1| - \rho_2 |s_2| - \rho_3 |s_3| - \rho_4 |s_4| \leq 0 \quad (65)$$

Therefore, the designed controller meets the Lyapunov stability condition, and it is proved that the whole system is asymptotically stable.

IV. SIMULINK RESULTS AND ANALYSIS

The main function of this section is to verify the effectiveness of the designed control strategy of the HESS system.

TABLE 1. Parameters of HESS model and adaptive terminal SMC.

Parameters	Value	
Model parameters	fuel cell	35-42Vdc,52A,46%
	battery	26.4Vdc,6.6Ah,Li-Ion
	supercapacitor	16Vdc,500F
	L_1, L_2, L_3	$3.3mH$
	R_1, R_2, R_3	$20m\Omega$
	C	$16mF$
Gains of controllers	ρ_1, ρ_2,	400000,100000
	ρ_3, ρ_4	150000,150000
Gains of sliding surface	k_1, k_2, k_3, k_4	0.1, 0.2, 0.2, 0.1
	p_1, p_2, p_3, p_4	5,5,5,5
	p_1, p_2, p_3, p_4	3,3,3,3
Gains of adaptive law	r_1, r_2, r_3	0.1,0.1,0.1

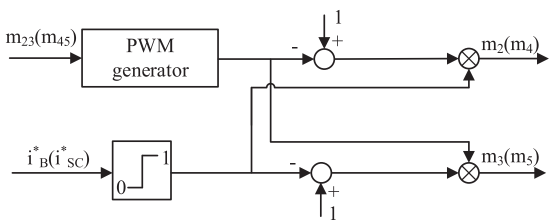

FIGURE 4. The generation of PWM signals m_2 and m_3 (m_4 and m_5).

The HESS in MATLAB/Simulink software environment is built. In Figure 3, the HESS can be shown in detail, whose values of model and adjustable parameters are summarized in Table 1. The generation of PWM signals m_2, m_3, m_4 and m_5 can be explained in Figure 4.

The simulation results of HESS can be shown as follows. In figure 5, the load required power is displayed, which simulates conditions of load in different cases. Meanwhile, the reference power and actual power are shown. When the P_{Load} is between 0W and 500W, which represents a small power load, the battery provides the full power because of high efficiency; when the P_{Load} is above 500W, fuel cell is

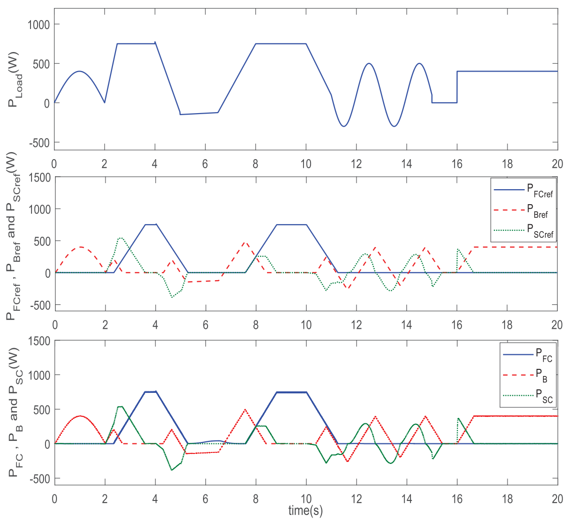

FIGURE 5. The power responses of FC, battery and SC.

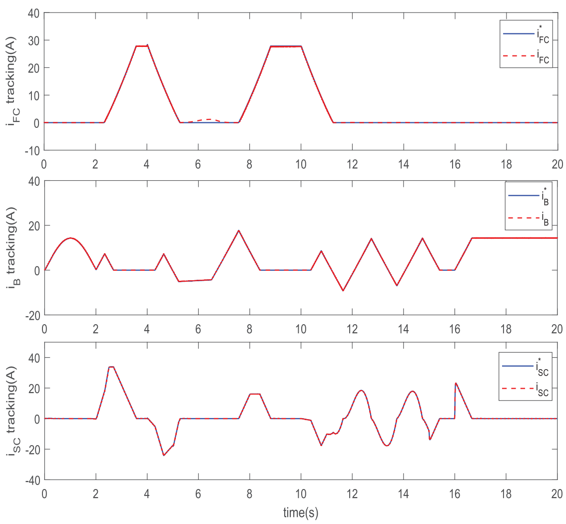

FIGURE 6. The tracking effect on FC, battery and SC reference current.

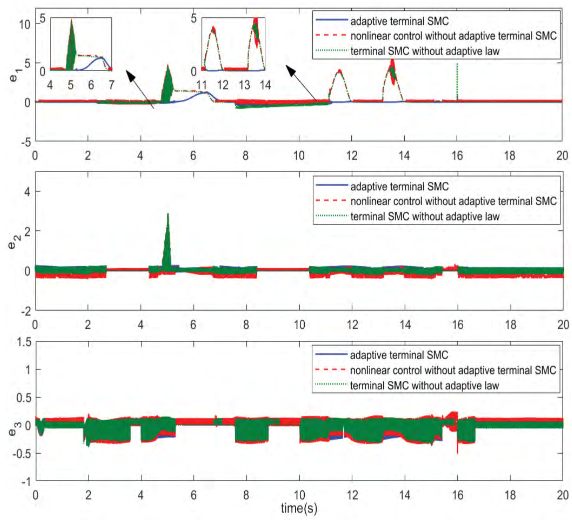

FIGURE 7. e_1, e_2 and e_3 comparison of three methods.

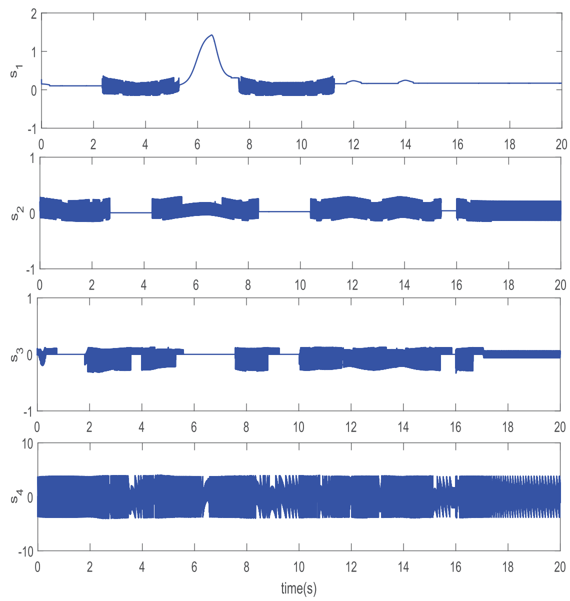

FIGURE 8. The time responses of the sliding functions s_1, s_2, s_3 and s_4.

responsible for full power supply; when it is less than 0W, it means the whole system absorbs energy from the outside, and the battery can be charged; when the peak power appears, FC and battery cannot provide power in time, then supercapacitor plays the main role. As the power type device, SC can provide power if the required power for the load increases or declines suddenly.

From figure 6, the tracking curves of i_{FC}, i_B and i_{SC} show the good performance of the designed controller, the current i_{FC}, i_B and i_{SC} can follow up $i_{FC}{}^*$, $i_B{}^*$ and $i_{SC}{}^*$ timely and accurately. Seen in figure 7, e_1, e_2 and e_3 of three methods are respectively compared. The good performance of the proposed control strategy is shown in e_1, especially in 4.5 to 7 seconds and 11 to 14 seconds, the curve of adaptive terminal SMC is better. And the e_2 of adaptive terminal SMC is smoother and more stable, especially around 5 seconds. In addition, the error e_3 obtained by three methods is almost stationary.

The robust convergence to the sliding surfaces can be seen in figure 8, which shows $s_i = 0,\ i = 1, 2, 3, 4$.

Figure 9 shows the overall variation of u_O, and the conclusion can be obtained that the DC bus voltage u_O stays around 50V. This shows the proposed control strategy can make the circuit generate the relatively stable voltage. Meanwhile, by comparing the u_O of adaptive terminal sliding mode control (adaptive terminal SMC), nonlinear control without adaptive terminal sliding mode control (nonlinear control without adaptive terminal SMC) and terminal sliding mode control without adaptive law (terminal SMC without

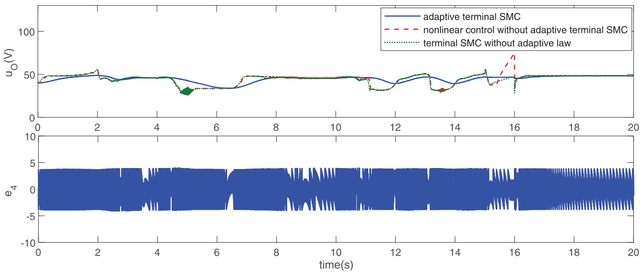

FIGURE 9. The DC link voltage u_O.

adaptive law), the result shows the effect of adaptive terminal SMC is better.

V. CONCLUSION

In this paper, a hybrid energy storage system is designed, which adopts the adaptive terminal sliding mode control. The control strategy contains two parts: (1) The power distribution strategy is proposed, which can distribute the load power reasonably and effectively, implement coordinated control of fuel cell, battery and supercapacitor. The combination of the three parts can meet the load power demand and maintain the stability of DC bus voltage at the same time. (2) Adaptive terminal sliding mode controller is designed. First, the terminal sliding mode can let the errors of reference and actual values approach zero in limited time. Then, the projection operator adaptive law is employed to estimate the unknown parameters of the model. The simulink results prove that the adaptive sliding mode control strategy has the advantages of fast response speed and good tracking performance. In future studies, the types and performance of fuel cell, battery and supercapacitor will be further studied. Meanwhile, in the case of system failure, the timely and effective compensation will be studied.

REFERENCES

[1] M. Gejguš, C. Aschbacher, and J. Sablik, "Comparison of the total costs of renewable and conventional energy sources," *Res. Papers Fac. Mater. Sci. Technol. Slovak Univ. Technol.*, vol. 24, no. 37, pp. 99–104, 2016.

[2] M. Dreidy, H. Mokhlis, and S. Mekhilef, "Inertia response and frequency control techniques for renewable energy sources: A review," *Renew. Sustain. Energy Rev.*, vol. 69, pp. 144–155, Mar. 2017.

[3] U. Desideri and J. Yan, "Clean energy technologies and systems for a sustainable world," *Appl. Energy*, vol. 97, no. 37, pp. 1–4, 2012.

[4] D. F. Dominković, I. Bačeković, A. S. Pedersen, and G. Krajačić, "The future of transportation in sustainable energy systems: Opportunities and barriers in a clean energy transition," *Renew. Sustain. Energy Rev.*, vol. 82, pp. 1823–1838, Feb. 2018.

[5] M. Aneke and M. Wang, "Energy storage technologies and real life applications—A state of the art review," *Appl. Energy*, vol. 179, pp. 350–377, Oct. 2016.

[6] N. Mahdavi, J. H. Braslavsky, M. M. Seron, and S. R. West, "Model predictive control of distributed air-conditioning loads to compensate fluctuations in solar power," *IEEE Trans. Smart Grid*, vol. 8, no. 6, pp. 3055–3065, Nov. 2017.

[7] M. Zidar, P. S. Georgilakis, N. D. Hatziargyriou, T. Capuder, and D. Škrlec, "Review of energy storage allocation in power distribution networks: Applications, methods and future research," *IET Generat., Transmiss. Distrib.*, vol. 10, no. 3, pp. 645–652, Mar. 2016.

[8] M. F. M. Sabri, K. A. Danapalasingam, and M. F. Rahmat, "A review on hybrid electric vehicles architecture and energy management strategies," *Renew. Sustain. Energy Rev.*, vol. 53, pp. 1433–1442, Jan. 2016.

[9] W. Gao, "Performance comparison of a fuel cell-battery hybrid powertrain and a fuel cell-ultracapacitor hybrid powertrain," *IEEE Trans. Veh. Technol.*, vol. 54, no. 3, pp. 846–855, May 2005.

[10] S. Zhang, R. Xiong, and J. Cao, "Battery durability and longevity based power management for plug-in hybrid electric vehicle with hybrid energy storage system," *Appl. Energy*, vol. 179, pp. 316–328, Oct. 2016.

[11] R. Hemmati and H. Saboori, "Emergence of hybrid energy storage systems in renewable energy and transport applications—A review," *Renew. Sustain. Energy Rev.*, vol. 65, pp. 11–23, Nov. 2016.

[12] J. Liu, Y. Gao, X. Su, M. Wack, and L. Wu, "Disturbance-observer-based control for air management of PEM fuel cell systems via sliding mode technique," *IEEE Trans. Control Syst. Technol.*, to be published. doi: 10.1109/TCST.2018.2802467.

[13] A. Aktas, K. Erhan, S. Ozdemir, and E. Ozdemir, "Experimental investigation of a new smart energy management algorithm for a hybrid energy storage system in smart grid applications," *Electric Power Syst. Res.*, vol. 144, pp. 185–196, Mar. 2017.

[14] F. Zhou, F. Xiao, C. Chang, Y. Shao, and C. Song, "Adaptive model predictive control-based energy management for semi-active hybrid energy storage systems on electric vehicles," *Energies*, vol. 10, no. 7, p. 1063, 2017.

[15] H. El Fadil, F. Giri, J. M. Guerrero, and A. Tahri, "Modeling and nonlinear control of a fuel cell/supercapacitor hybrid energy storage system for electric vehicles," *IEEE Trans. Veh. Technol.*, vol. 63, no. 7, pp. 3011–3018, Sep. 2014.

[16] A. Castaings, W. Lhomme, R. Trigui, and A. Bouscayrol, "Comparison of energy management strategies of a battery/supercapacitors system for electric vehicle under real-time constraints," *Appl. Energy*, vol. 163, pp. 190–200, Feb. 2016.

[17] L. Wang, Y. Han, X. Feng, J. Zhou, P. Qi, and B. Wang, "Metal–organic frameworks for energy storage: Batteries and supercapacitors," *Coordination Chem. Rev.*, vol. 307, pp. 361–381, Jan. 2016.

[18] J. Li *et al.*, "Toward low-cost, high-energy density, and high-power density lithium-ion batteries," *J. Minerals*, vol. 69, no. 9, pp. 1484–1496, 2017.

[19] H. Armghan, I. Ahmad, N. Ali, M. F. Munir, S. Khan, and A. Armghan, "Nonlinear controller analysis of fuel cell–battery–ultracapacitor-based hybrid energy storage systems in electric vehicles," *Arabian J. Sci. Eng.*, vol. 43, no. 6, pp. 3123–3133, 2018.

[20] L. Solero, A. Lidozzi, and J. A. Pomilio, "Design of multiple-input power converter for hybrid vehicles," *IEEE Trans. Power Electron.*, vol. 20, no. 5, pp. 1007–1016, Sep. 2005.

[21] Q. Zhang, W. W. Deng, and G. Li, "Stochastic control of predictive power management for battery/supercapacitor hybrid energy storage systems of electric vehicles," *IEEE Trans. Ind. Informat.*, vol. 14, no. 7, pp. 3023–3030, Jul. 2018.

[22] J. Li, R. Xiong, Q. Yang, F. Liang, M. Zhang, and W. Yuan, "Design/test of a hybrid energy storage system for primary frequency control using a dynamic droop method in an isolated microgrid power system," *Appl. Energy*, vol. 201, pp. 257–269, Sep. 2017.

[23] J. W. Li, Q. Q. Yang, F. Robinson, F. Liang, M. Zhang, and W. Yuan, "Design and test of a new droop control algorithm for a SMES/battery hybrid energy storage system," *Energy*, vol. 118, pp. 1110–1122, Jan. 2017.

[24] W. Zhang, D. Xu, X. Lou, W. Yan, and W. Yang, "Power management of battery energy storage system using model free adaptive control," in *Proc. IEEE 7th Data Driven Control Learn. Syst. Conf. (DDCLS)*, May 2018, pp. 798–801.

[25] L. Wu, W. X. Zheng, and H. Gao, "Dissipativity-based sliding mode control of switched stochastic systems," *IEEE Trans. Autom. Control*, vol. 58, no. 3, pp. 785–791, Mar. 2013.

[26] F. Li, L. Wu, P. Shi, and C.-C. Lim, "State estimation and sliding mode control for semi-Markovian jump systems with mismatched uncertainties," *Automatica*, vol. 51, pp. 385–393, Jan. 2015.

[27] S. K. Gudey and R. Gupta, "Recursive fast terminal sliding mode control in voltage source inverter for a low-voltage microgrid system," *IET Gener., Transmiss. Distrib.*, vol. 10, no. 7, pp. 1536–1543, 2016.

[28] A. M. Shotorbani, S. Ghassem-Zadeh, B. Mohammadi-Ivatloo, and S. H. Hosseini, "A distributed secondary scheme with terminal sliding mode controller for energy storages in an islanded microgrid," *Int. J. Elect. Power Energy Syst.*, vol. 93, pp. 352–364, Dec. 2017.

[29] Z. Song *et al.*, "Sliding-mode and Lyapunov function-based control for battery/supercapacitor hybrid energy storage system used in electric vehicles," *Energy*, vol. 122, pp. 601–612, Mar. 2017.

[30] C. Hu, Z. Wang, Y. Zhu, M. Zhang, and H. Liu, "Performance-oriented precision LARC tracking motion control of a magnetically levitated planar motor with comparative experiments," *IEEE Trans. Ind. Electron.*, vol. 63, no. 9, pp. 5763–5773, Sep. 2016.

[31] P. K. Anh and N. T. Vinh, "Self-adaptive gradient projection algorithms for variational inequalities involving non-Lipschitz continuous operators," *Numer. Algorithms*, pp. 1–19, Aug. 2018. doi: 10.1007/s11075-018-0578-z.

[32] S. Lee, M. Park, and J. Baek, "Robust adaptive synchronization of a class of chaotic systems via fuzzy bilinear observer using projection operator," *Inf. Sci.*, vol. 402, pp. 182–198, Sep. 2017.

[33] D. Xu, B. Jiang, and P. Shi, "A novel model-free adaptive control design for multivariable industrial processes," *IEEE Trans. Ind. Electron.*, vol. 61, no. 11, pp. 6391–6398, Nov. 2014.

[34] D. Xu, B. Jiang, and P. Shi, "Adaptive observer based data-driven control for nonlinear discrete-time processes," *IEEE Trans. Autom. Sci. Eng.*, vol. 11, no. 4, pp. 1037–1045, Oct. 2014.

[35] W. Sun, Y. Zhang, Y. Huang, H. Gao, and O. Kaynak, "Transient-performance-guaranteed robust adaptive control and its application to precision motion control systems," *IEEE Trans. Ind. Electron.*, vol. 63, no. 10, pp. 6510–6518, Mar. 2016.

[36] B. Jiang, D. Xu, P. Shi, and C. C. Lim, "Adaptive neural observer-based backstepping fault tolerant control for near space vehicle under control effector damage," *IET Control Theory Appl.*, vol. 8, no. 9, pp. 658–666, 2014.

[37] J. Yao, Z. Jiao, and D. Ma, "A practical nonlinear adaptive control of hydraulic servomechanisms with periodic-like disturbances," *IEEE/ASME Trans. Mechatronics*, vol. 20, no. 6, pp. 2752–2760, Dec. 2015.

[38] J. Yao and W. Deng, "Active disturbance rejection adaptive control of hydraulic servo systems," *IEEE Trans. Ind. Electron.*, vol. 64, no. 10, pp. 8023–8032, Oct. 2017.

DEZHI XU received the Ph.D. degree in control theory and control engineering from the Nanjing University of Aeronautics and Astronautics, China, in 2013. He joined Jiangnan University, Wuxi, China, as an Associate Professor and a Master Tutor. His research interests include data-driven control, fault diagnosis and fault-tolerant control, technologies of renewable energy, and smart grid. He is a member of the IEEE. He is also a Committee Member of the Association of Energy Internet, CAA. His research results as important components received the First Class Award of Science and Technology Progression from the China General Chamber of Commerce, in 2016.

QIAN LIU is currently pursuing the master's degree with the School of Internet of Things Engineering, Jiangnan University. Her research interest includes nonlinear control in energy storage systems.

WENXU YAN received the M.S. and Ph.D. degrees from Jiangnan University, Wuxi, China, where he is currently an Associate Professor with the School of Internet of Things Engineering. His current research interests include adaptive control theory and application, renewable energy, and smart grid. He is a member of the IEEE.

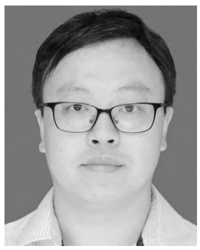

WEILIN YANG received the B.Eng. degree in machine design and manufacture and their automation from the University of Science and Technology of China, Hefei, China, in 2009, and the Ph.D. degree in mechanical engineering from the City University of Hong Kong, Hong Kong, in 2009.

He was a Postdoctoral Researcher with the Masdar Institute of Science and Technology, Abu Dhabi, United Arab Emirates, from 2013 to 2016. He was a Research Engineer with General Electric Global Research, Shanghai, from 2016 to 2017. He has been an Assistant Professor with Jiangnan University, since 2017. His research interests include modeling and control of energy systems and computational fluid dynamics.

Dr. Yang is a member of the IEEE.